Preparation of the layered double hydroxide (LDH) $LiAl_2(OH)_7{\cdot}2H_2O$, by gel to crystallite conversion and a hydrothermal method, and its conversion to lithium aluminates

M. Nayak,[a] T. R. N. Kutty,*[a] V. Jayaraman[b] and G. Periaswamy,[b]

[a]*Materials Research Centre, Indian Institute of Science, Bangalore 560 012, India*

[b]*Materials Chemistry Division, Indira Gandhi Centre for Atomic Research, Kalpakkam 603 102, India*

A layered double hydroxide (LDH) with chemical composition $LiAl_2(OH)_7{\cdot}2H_2O$ was prepared *via* a wet chemical route of gel to crystallite (G–C) conversion at 80 °C involving the reaction of hydrated alumina gel, $Al_2O_3{\cdot}yH_2O$ ($80 < y < 120$) with LiOH ($Li_2O/Al_2O_3 \geqslant 0.5$) in presence of hydrophilic solvents such as ethanol under refluxing conditions. The hydrothermal synthesis was carried out using the same reactants by heating to $\leqslant 140$ °C in a Teflon-lined autoclave under autogenerated pressure ($\leqslant 20$ MPa). Transmission electron microscopy showed needle-shaped aggregates of size 0.04–0.1 μm for the gel to crystallite conversion product, whereas the hydrothermal products consisted of individual lamellar crystallites of size 0.2–0.5 μm with hexagonal morphology. The LDH prepared through the gel to crystallite conversion could be converted into $LiAl(OH)_4{\cdot}H_2O$ or $LiAl(OH)_3NO_3{\cdot}H_2O$ by imbibition of LiOH or $LiNO_3$, respectively, under hydrothermal conditions. Thermal decomposition of LDH above 1400 °C gave rise to $LiAl_5O_8$ accompanied by the evaporation of Li_2O. $LiAl(OH)_4{\cdot}H_2O$ and $LiAl(OH)_3NO_3{\cdot}H_2O$ decomposed in the temperature range 400–1000 °C to α- or β-$LiAlO_2$. The compositional dependence of the product, the intermediate phases formed during the heat treatment and the possible reactions involved are described in detail.

The compounds $LiAl_5O_8$ and $LiAlO_2$ are luminescent hosts when doped with Fe^{3+}, emitting in the red spectral region.[1,2] These red-emitting phosphors are useful for artificial illumination in plant growth applications.[2–4] One of the polymorphic forms of $LiAlO_2$, *viz.* γ-$LiAlO_2$, has received much attention because of the possibility of its use as a tritium breeding material in fusion reactors[5,6] and as an electrolyte matrix for molten carbonate fuel cells.[7,8] High surface area α-$LiAlO_2$ is used as a catalyst support[9] and for the preparation of the delithiated transitional alumina compounds.[10] The present work aims to decipher routes to obtain phase-pure $LiAlO_2$ (different polymorphic forms) and $LiAl_5O_8$ wherein LDH [$LiAl_2(OH)_7{\cdot}2H_2O$] is used as a precursor and also has many applications of its own. Layered lithium dialuminium hydroxide, $LiAl_2(OH)_7{\cdot}2H_2O$, which is analogous to the mineral hydrotalcite, $[Mg_6Al_2(OH)_{16}]CO_3{\cdot}4H_2O$, has received a lot of attention because of its potential application in the field of sensors, and also as antacid, by way of selective sorption of weak acids (H_2S, CO_2, *etc.*,). It also finds uses in ion exchange for poisonous anions such as $[Fe(CN)_6]^{4-}$, solid-state anion conductors and in catalysis.[11–17] Moreover, the compound is a precursor for the preparation of $LiAl_5O_8$ and $LiAlO_2$.

A number of publications exist in the literature on the synthesis and physicochemical properties of these compounds.[1–17] Poppelmeir *et al.*[17] prepared $LiAl_2(OH)_7{\cdot}2H_2O$ by the insertion of LiOH into $Al(OH)_3$ and studied the phase relations and stability of the compounds at different temperature regimes. Their papers do not deal with the phases stabilised at temperatures >1200 °C and the possible conversion of $LiAlO_2$ to $LiAl_5O_8$. The difficulty in the imbibition technique to maintain the Li_2O/Al_2O_3 molar ratio, often leads to the presence of unreacted reactants and phase purity is difficult to attain. Most of the literature is on the ion exchange, intercalation products and the possible applications thereof. We prepared $LiAl_2(OH)_7{\cdot}2H_2O$ through the novel route of gel to crystallite (G–C) conversion[18–20] as well as *via* a hydrothermal method,[21–23] which acted as a precursor for the preparation of $LiAlO_2$ and $LiAl_5O_8$. The advantages of the G–C conversion include procedural simplicity and economy of the method as the starting materials are cheap water-soluble inorganic salts. The gel can be converted directly to crystallites in the presence of an organic solvent owing to instability of the gel caused by influx of aliovalent ions. The merits of this process over the conventional ceramic processing are the increased homogeneity of the products and the reduction in the processing temperature. G–C conversion can take place even with coarser gels so that the raw materials need not include expensive organometallics or alkoxides. The general reaction involved in this technique is the breakdown of the gel network owing to the ionic pressure caused by the influx of aliovalent ions. Hydrothermal synthesis is based on supersaturated solvents under elevated pressure–temperature (P–T) conditions; accordingly the end product may differ.

Experimental

The principle involved and the experimental details of G–C conversion technique have been presented in our previous publications.[18–20] Hydrated alumina gel was prepared through precipitating Al^{3+} (aq) with 30 mass% ammonia solution, washed free of anion contaminants using hot water (tested for the absence of sulfate by adding $Ba(OH_2)$ solution and for chloride ions by adding $AgNO_3$ solution to the filtrate) and suspended in a conical flask containing ethanolic lithium hydroxide. The presence of anionic contaminants such as SO_4^{2-} and Cl^- impedes the reaction. The reaction vessel was fitted with a water-cooled condenser and an alkali guard tube to prevent the ingress of CO_2 and refluxed for 5–6 h at 80 °C while continuously stirring using a magnetic stirrer. The solid product obtained was washed free of unreacted LiOH and air-dried in a desiccator. The lithium content in the washings was monitored to measure the extent of reaction and to compare the composition of the solid product obtained *via* the wet-chemical route (AAS).

Hydrothermal preparation was carried out in a Teflon (PTFE)-lined Morey-type autoclave SS318. The autoclave was charged with the reactants, *viz.* hydrated alumina gel mixed with LiOH in the desired molar ratio; deionised water was added to the required percentage so as to autogenerate pressure in the range 5–40 MPa and heated in the temperature range

100–240 °C for 12 h. The temperature was varied to check the phase stability region. Hydrothermal imbibition was performed by charging the autoclave with previously prepared LDH and LiOH or $LiNO_3$ in the desired molar ratio. Imbibition was carried out at 140 °C for 12 h.

The chemical compositions of the products were determined by wet chemical analyses using atomic absorption spectroscopy (AAS). Thermal analyses were performed on a simultaneous thermogravimetry–differential thermal analysis (TG–DTA) instrument from Polymer Laboratory STA-1500 at a heating rate of 5 °C min^{-1}. Phase identification of the powders was carried out by X-ray powder diffraction using a Scintag/USA diffractometer. IR absorption spectra were recorded on a BIORAD FTIR spectrometer in the range 4000–400 cm^{-1}. Solid-state ^{27}Al MAS NMR spectra were obtained at 78.2 MHz using a high-resolution NMR spectrometer (BRUKER 300 MHz) at room temperature fitted with a magic angle spinning probe (MAS) for rotating the sample at a frequency of 7 kHz. ^{27}Al MAS NMR chemical shifts (δ) were referenced to 1 M $Al(H_2O)_6Cl_3$ ($\delta = 0$). The morphology and the particle size were determined by the intercept method on the micrographs obtained from a JEOL 200 CX, 200 kV transmission electron microscope (TEM) having 2 Å resolution.

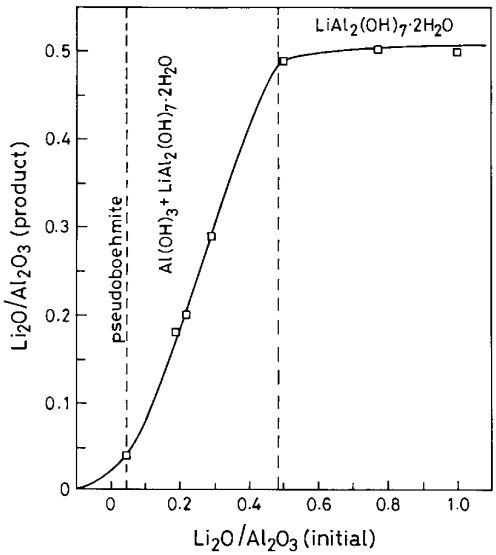

Fig. 1 Variation of Li_2O/Al_2O_3 molar ratio in the product as a function of initial Li_2O/Al_2O_3 molar ratio in the reaction mixture

Results and Discussion

Gel to crystallite conversion

Effect of initial composition on phase formation. The composition of the solid phases prepared through G–C conversion were dependent on the initial Li_2O/Al_2O_3 mol ratio in the reaction mixture (Fig. 1). It is evident that as the Li_2O/Al_2O_3 ratio is increased in the reaction mixture, the lithium retained in the product is also increased and attained a limiting value of *ca.* 0.5. Above this concentration, the excess lithium added was washed out. Table 1 gives the chemical composition of the as-prepared samples for various starting ratios and the resultant products on subsequent heat treatment at 900 or above 1400 °C. At $Li_2O/Al_2O_3 \leqslant 0.05$, the phase formed is pseudoboehmite which decomposed on heat treatment to give α-Al_2O_3 and $LiAl_5O_8$. For Li_2O/Al_2O_3 ratios between 0.05 and 0.5, a mixture of nordstrandite [$Al(OH)_3$] and $LiAl_2(OH)_7{\cdot}2H_2O$ was formed. Above a Li_2O/Al_2O_3 ratio of 0.5, a voluminous mass having the chemical composition $LiAl_2(OH)_7{\cdot}2H_2O$ was obtained. The formation of LDH is confirmed by X-ray diffraction (XRD) (Fig. 4, later). Preparing a phase of composition $LiAl(OH)_4{\cdot}H_2O$ was not possible *via* this route owing to leaching of LiOH.

Thermal analyses. Fig. 2 shows thermal analyses traces of $LiAl_2(OH)_7{\cdot}2H_2O$ prepared by G–C conversion. The sample showed a total mass loss of 53% up to 540 °C in agreement with the literature,[17] however the sequence of mass losses differ. The TG curve shows that the major mass loss occurred below 540 °C in three steps. The initial mass loss (5%) below 100 °C is probably due to the loss of physically absorbed water.

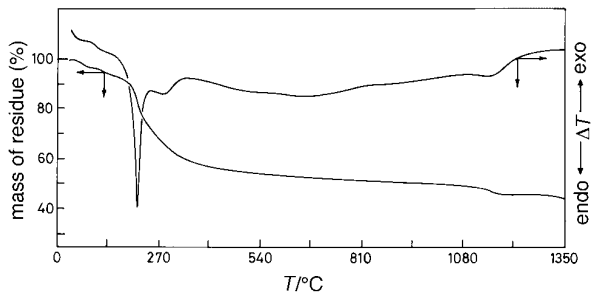

Fig. 2 TG–DTA traces of $LiAl_2(OH)_7{\cdot}2H_2O$ prepared through G–C conversion

A mass loss (16%) between 100 and 200 °C accompanied by a very strong endothermic peak in the DTA is due to the removal of structural water. Between 200 and 500 °C, the mass loss is *ca.* 32% which can be attributed to dehydroxylation. DTA shows a corresponding broad and shallow endotherm centred around 270 °C. A subsequent endotherm at 640 °C accompanied by a mass loss of 6% is due to the dehydroxylation of the residual hydroxy groups. Continuous mass loss between 1000 and 1300 °C, and the endotherm which shows a peak at 1143 °C, is due to the evaporation of Li_2O. Samples prepared at higher initial Li_2O/Al_2O_3 ratios (>0.5) show the same trends as above during thermal analyses.

Isothermal mass loss measurements were also carried out at various temperatures until a constant mass was obtained and the results are in good agreement with the dynamic mass loss

Table 1 Chemical compositions of the as-prepared LDH and the phases obtained upon calcination above 1400 °C

Li_2O/Al_2O_3 molar ratio			after calcination at	
reaction mixture	product	as-prepared	900 °C	1400 °C
0.05	0.04	pseudoboehmite	α-$Al_2O_3 + LiAl_5O_8$	α-$Al_2O_3 + LiAl_5O_8$
0.19	0.18	$Al(OH)_3 + LiAl_2(OH)_7{\cdot}2H_2O$	γ-$LiAlO_2 + LiAl_5O_8$	γ-$LiAlO_2 + LiAl_5O_8$
0.22	0.2	$Al(OH)_3 + LiAl_2(OH)_7{\cdot}2H_2O$	$LiAl_5O_8$	$LiAl_5O_8$
0.29	0.29	$Al(OH)_3 + LiAl_2(OH)_7{\cdot}2H_2O$ (major)	γ-$LiAlO_2 + LiAl_5O_8$	$LiAl_5O_8$
0.5	0.49	$LiAl_2(OH)_7{\cdot}2H_2O$	γ-$LiAlO_2 + LiAl_5O_8$	$LiAl_5O_8$
0.72	0.49	$LiAl_2(OH)_7{\cdot}2H_2O$	γ-$LiAlO_2 + LiAl_5O_8$	$LiAl_5O_8$
1	0.5	$LiAl_2(OH)_7{\cdot}2H_2O$	γ-$LiAlO_2 + LiAl_5O_8$	$LiAl_5O_8$

measurements. Static mass loss measurements shows a total Δm of *ca.* 58% between room temperature and 1300 °C.

Based on the thermal analyses results, the following reaction scheme can be proposed for the formation of $LiAl_5O_8$ from $LiAl_2(OH)_7{\cdot}2H_2O$:

$$LiAl_2(OH)_7{\cdot}2H_2O \xrightarrow{150\,^\circ C} LiAl_2(OH)_7 + 2H_2O \quad \Delta m = 17\% \quad (1)$$

$$LiAl_2(OH)_7 \xrightarrow{500\,^\circ C} LiAl_2O_3(OH) + 3\ H_2O \quad \Delta m = 30\% \quad (2)$$

$$4\ LiAl_2O_3(OH) \xrightarrow{600\,^\circ C} 2\ 'Li_2Al_4O_7' + 2H_2O \quad \Delta m = 7\%$$

$$(\equiv 3\ LiAlO_2 + LiAl_5O_8) \quad (3)$$

$$5\ LiAlO_2 \xrightarrow[24\ h]{1400\,^\circ C} LiAl_5O_8 + 2Li_2O\uparrow \quad \Delta m = 18\% \quad (4)$$

IR absorption spectra. Samples isolated from the isothermal mass loss studies were analysed by IR absorption spectra for the presence of hydroxy groups in the intermediates. Fig. 3 shows the IR absorption spectra of the sample as a function of temperature. The sample heated to 105 °C shows a broad absorption band centred around 3450 cm^{-1} owing to the O—H stretching frequencies from hydrogen bonded as well as bridged hydroxy groups. Sharp peaks at 1025, 825 and 550 cm^{-1} and shoulders at 675 and 650 cm^{-1} are characteristics of AlO_6 octahedra. On heating the sample to 250 °C, the peak at 3450 cm^{-1} is considerably reduced in intensity, indicating that the hydroxy groups are removed from the sample. Also, the peak at 1375 cm^{-1} vanishes, and a doublet appears at *ca.* 1550 cm^{-1}. A new peak was observed at 1200 cm^{-1}. Also, the number of peaks between 1000 and 500 cm^{-1} reduces to one (centred around 550 cm^{-1}). When the sample was heated at 800 °C, the absorption band at 3450 cm^{-1} was completely lost indicating the disappearance of all hydroxy groups. On further heating at 1400 °C, sharp multiple bands were observed between 1000 and 400 cm^{-1}. These sharp peaks are attributed to AlO_6 groups.[24]

X-Ray diffraction. XRD patterns as a function of calcination temperature are shown in Fig. 4. An oven dried (105 °C) sample does not show any difference in its XRD pattern compared with as-prepared specimens. The sample annealed at 150 °C shows a similar pattern but with broadened diffraction peaks and diminished intensity. The reason for this is the removal of interlayer water, a fact confirmed by TG–DTA studies and IR absorption spectra. Further heating of the sample to 250 °C, resulted in a complete change of the diffraction pattern, which consists of very broad and weak diffraction peaks corresponding to $LiAlO_2$ with small crystallite size. The change in the XRD pattern is due to the complete destruction of brucite type layers. As the temperature of calcination is increased to 450 °C, β-$LiAlO_2$ started nucleating, and become a major phase at 600 °C. At 1000 °C the phases stablised are γ-$LiAlO_2$ (major) and $LiAl_5O_8$ (minor). Upon further increase in temperature, γ-$LiAlO_2$ decomposed and the formation of $LiAl_5O_8$ was favoured. This change is associated with the evaporation of lithia, Li_2O, as detected from the effluent gas when purged with dry argon while the sample is heated in a tubular furnace. Prolonged heat treatment above 1400 °C yielded monophasic $LiAl_5O_8$. Further phase separation occurred on raising the temperature above 1600 °C. The resultant phases are α-Al_2O_3(minor) and $LiAl_5O_8$.

Hydrothermal preparation of $LiAl_2(OH)_7{\cdot}2H_2O$

The products from the hydrothermal preparative runs are shown in Table 2. The temperature of the hydrothermal treatment was varied in order to study the conditions of preparation at which the phase is stable. Essentially, our results indicate that, along with the composition, *P–T* conditions have great influence on the phase stability. LDH is stabilised only if

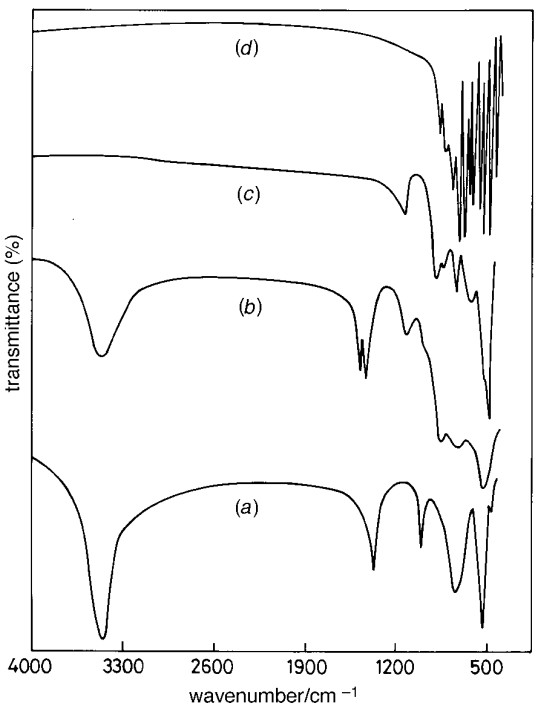

Fig. 3 IR spectra of $LiAl_2(OH)_7{\cdot}2H_2O$ as a function of temperature: (*a*) 105 °C, (*b*) 250 °C, (*c*) 1000 °C and (*d*) 1400 °C

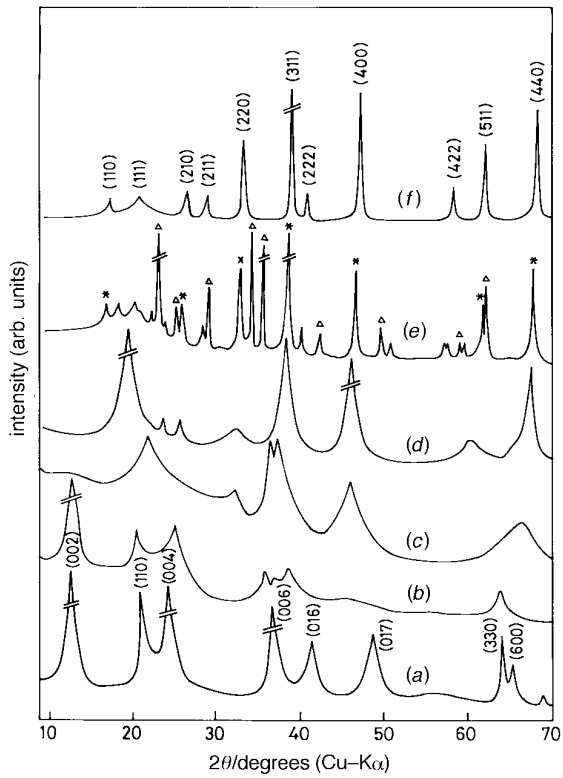

Fig. 4 XRD traces of the $LiAl_2(OH)_7{\cdot}2H_2O$ as a function of temperature: (*a*) 105 °C, (*b*) 150 °C, (*c*) 250 °C, (*d*) 450 °C, (*e*) 1000 °C and (*f*) 1400 °C (△, γ-$LiAlO_2$; *, $LiAl_5O_8$)

Table 2 Results of the hydrothermal preparative runs at three different temperatures

Li_2O/Al_2O_3 in the reaction mixture	as-prepared		
	140 °C	180 °C	240 °C
1	$LiAl_2(OH)_7{\cdot}2H_2O$	β-$LiAlO_2$ + γ-AlOOH	β-$LiAlO_2$
0.5	$LiAl_2(OH)_7{\cdot}2H_2O$	β-$LiAlO_2$ + γ-AlOOH	β-$LiAlO_2$ + γ-AlOOH
0.33	$LiAl_2(OH)_7{\cdot}2H_2O$ + γ-AlOOH	γ-AlOOH	γ-AlOOH
0.25	γ-AlOOH + $LiAl_2(OH)_7{\cdot}2H_2O$	γ-AlOOH	γ-AlOOH
0.2	γ-AlOOH	γ-AlOOH	γ-AlOOH

$Li_2O/Al_2O_3 \geqslant 0.5$, at temperatures below 140 °C. Larger crystallite size ($\leqslant 0.5$ μm) and better crystallinity were obtained using higher concentrations of LiOH. As the temperature of the hydrothermal preparation was increased above 150 °C, irrespective of the composition, the phases stabilised were β-$LiAlO_2$ + γ-AlOOH (boehmite) at $Li_2O/Al_2O_3 \geqslant 0.5$ and only boehmite at $Li_2O/Al_2O_3 < 0.5$. Pure phase β-$LiAlO_2$ was obtained for $Li_2O/Al_2O_3 = 1$ at a temperature $\geqslant 240$ °C.

Fig. 5 shows the X-ray diffraction patterns of LDH prepared through the hydrothermal route at 140 °C. All the diffraction peaks due to the basal planes are split, as a result of anion insertion in the intermediate layer. Diffraction peaks arising from the (330) and (600) reflections are totally absent. Fig. 5 (inset) shows enlarged portions of (002) and (004) reflections. On increasing the lithium concentration, the extent of splitting was not very much increased.

DTA traces of the hydrothermal products (Fig. 6) show multiple thermal events in the temperature range 30–400 °C unlike the G–C prepared sample. Sharp endotherms at 46 and 77 °C are due to the desorption of water and endotherms at 132 and 192 °C arise from the removal of interlayer water. XRD analysis shows diminished intensity of all the basal

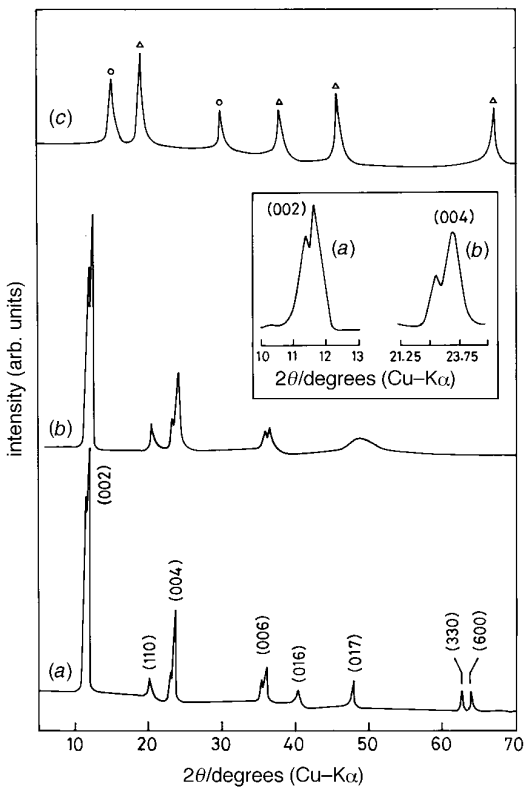

Fig. 5 XRD patterns of $LiAl_2(OH)_7{\cdot}2H_2O$ prepared *via* the hydrothermal route at 140 °C with initial Li_2O/Al_2O_3 ratios of (*a*) 1, (*b*) 0.5 and (*c*) sample on further imbibition with LiOH. Inset shows the enlarged portions of the basal reflections of hydrothermally prepared samples (*a*) (002) and (*b*) (004). (○, Boehmite; △, α-$LiAlO_2$).

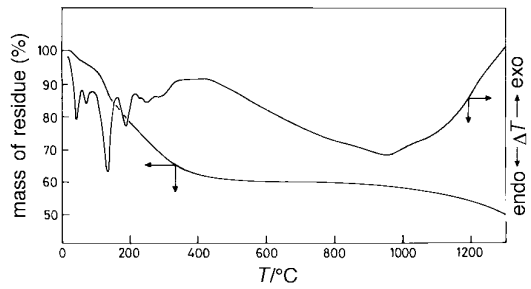

Fig. 6 TG–DTA traces of $LiAl_2(OH)_7{\cdot}2H_2O$ prepared *via* the hydrothermal route

planes and the peaks are broadened accompanied by a shift to higher angles, yet retaining the LDH pattern. Shallow, broad endotherms at 250 and 275 °C arise from the removal of hydroxy groups attached to the Al and Li in the brucite type layers. X-Ray analysis of the heat-treated sample showed a completely amorphous pattern. A very broad and shallow endotherm centred around 950 °C is due to the loss of residual hydroxy groups; the phases formed thereupon are mixtures of γ-$LiAlO_2$ and $LiAl_5O_8$. The intermediate phases, on heat treatment, are the same as that of the sample prepared through G–C conversion; above 1400 °C the phase stabilised is $LiAl_5O_8$.

Table 3 shows TG data of the intermediate products formed. TG curves indicate that the major mass loss occurred below 500 °C. Between 500 and 1050 °C, the mass loss is only 3% owing to removal of residual hydroxy groups. The continuous mass loss above 1050 °C without any thermal events is due to the evaporation of Li_2O which is responsible for the formation of $LiAl_5O_8$ above 1400 °C, according to reaction (4).

Hydrothermal imbibition to prepare $LiAl(OH)_4{\cdot}H_2O$

To achieve higher Li_2O/Al_2O_3 molar ratios in the LDH prepared through G–C conversion or hydrothermally, samples were further hydrothermally imbibed with LiOH and $LiNO_3$ at 140 °C. Hydrothermal imbibition of LiOH into the LDH prepared through the hydrothermal route resulted in the formation of α-$LiAlO_2$ and boehmite (γ-AlOOH) [Fig. 5(*c*)]. Further insertion of LiOH created instability in the compound resulting in phase separation into α-$LiAlO_2$ and boehmite. In

Table 3 TG analyses data of the LDH prepared through hydrothermal route at 140 °C and the intermediate phases stabilised

temperature/°C	mass loss (%)	phase formed
RT–100 °C	6	$LiAl_2(OH)_7{\cdot}2H_2O$
100–200 °C	17	$LiAl_2(OH)_7{\cdot}2H_2O$ (intensity of all the basal diffraction peaks diminished)
200–500 °C	30	very broad peaks corresponding to α-$LiAlO_2$, amorphous background indication of poorly crystallised second phase
500–1050 °C	3	β-$LiAlO_2$ + $LiAl_5O_8$
1050–1300 °C	7	$LiAl_5O_8$ + γ-$LiAlO_2$

contrast, G–C prepared samples allow imbibition. The imbibed sample has a Li_2O/Al_2O_3 ratio of *ca.* 1, corresponding to the composition $LiAl(OH)_4{\cdot}H_2O$. Fig. 7 shows the XRD patterns of the imbibed samples in relation to the starting composition (G–C prepared). The major difference is that some of the basal reflections, (004) and (006), are split, whereas splitting is not observed for (002) reflection. The splitting of the XRD peaks is due to the insertion of $LiNO_3$, LiOH or $[Li(OH)_2]^-$ ions into the intermediate layer. Splitting is not very pronounced for $LiNO_3$ imbibed samples, whereas LiOH inserted samples show clear splittings. On further increase of LiOH, the phases stabilised are $LiAl_2(OH)_7{\cdot}2H_2O$ and β-$LiAlO_2$. Table 4 summarises the decomposition products of these compositions and the polymorphic forms of $LiAlO_2$ stabilised at different temperatures. The decomposition product is γ-$LiAlO_2$ which is a luminescent host for Fe^{3+} ions having an emission maximum at *ca.* 708 nm.

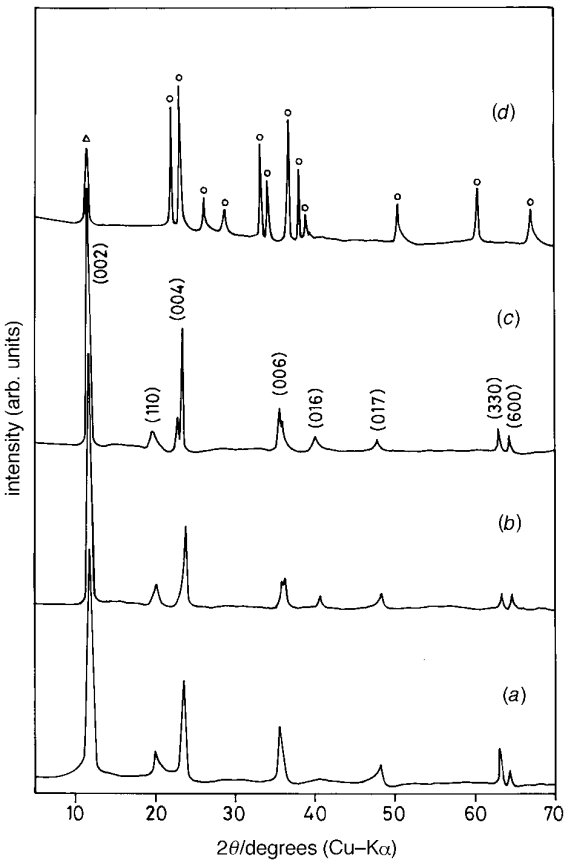

Fig. 7 XRD tracings of the hydrothermally imbibed samples: (*a*) as-prepared $LiAl_2(OH)_7{\cdot}2H_2O$ prepared through G–C conversion; (*b*) imbibed with $LiNO_3$; (*c*) imbibed with LiOH, LDH/LiOH = 1; (*d*) imbibed with LiOH, LDH/LiOH = 0.5 [LDH = $LiAl_2(OH)_7{\cdot}2H_2O$]; ○, β-$LiAlO_2$; △, $LiAl_2(OH)_7{\cdot}2H_2O$

IR absorption spectra (Fig. 8) of the imbibed samples show clear differences from that of the starting composition in terms of the intensity and sharpness of the absorption bands for the LiOH imbibed sample and splitting of the bands and broadening are observed for the $LiNO_3$ imbibed sample. However, the essential pattern is the same, indicating that the basic structure remains undisturbed. Both samples show absorption due to hydrogen-bonded, bridged hydroxy groups similar to that of the starting composition. The LiOH imbibed sample shows a very strong and sharp peak at 1380 cm^{-1} band and the shoulders at 1618 and 1491 cm^{-1} almost the same as in the starting material. A gain in intensity of the 1380 cm^{-1} band is due to the intercalation of $Li(OH)_2^-$ in the intermediate layer. An increase in sharpness as well as the absorption intensity beyond 1000 cm^{-1} (characteristics of the AlO_6 group) indicate cation ordering in the octahedral sites. In contrast, insertion of $LiNO_3$ leads to intensification of bands at 1618, 1491 (clearly split) and 1380 cm^{-1} along with a new band at 1436 cm^{-1} corresponding to the asymmetric stretching of the NO_3^- group (ν_3) while the absorption band due to symmetric stretching (ν_1) is observed at 1112 cm^{-1}; absorption bands beyond 1000 cm^{-1} are much broadened.

^{27}Al MAS NMR spectra of different polymorphs of $LiAlO_2$ are shown in Fig. 9. The polymorphs show clear differences in chemical shift. The low temperature form (<400 °C) of α-$LiAlO_2$ shows a chemical shift of δ 9.5 corresponding to ^{27}Al

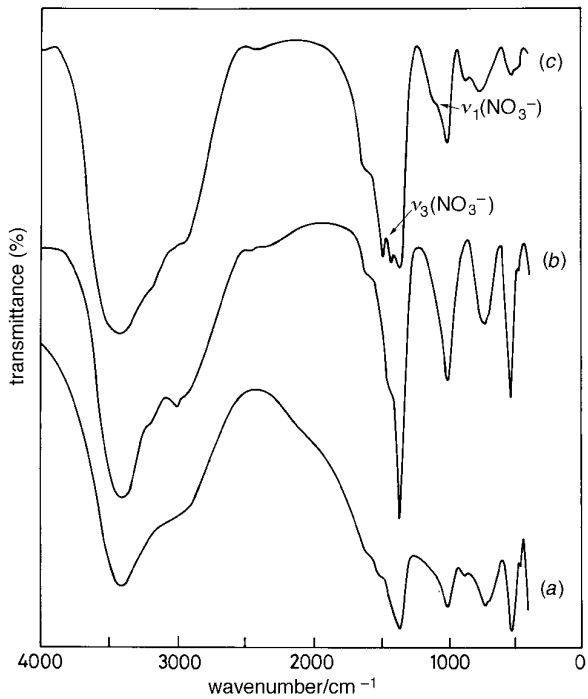

Fig. 8 IR spectra of $LiAl_2(OH)_7{\cdot}2H_2O$: (*a*) before imbibition, (*b*) imbibition with LiOH and (*c*) imbibition with $LiNO_3$

Table 4 Phases prepared through hydrothermal imbibition of $LiAl_2(OH)_7$ prepared through G–C conversion and the polymorphic forms of $LiAlO_2$

composition of the charge	as-prepared	400 °C	500 °C	1000 °C	1300 °C
LDH : 1$LiNO_3$	$LiAl(OH)_3NO_3{\cdot}H_2O$	α-$LiAlO_2$	β-$LiALO_2$	γ-$LiAlO_2$	γ-$LiAlO_2$
LDH : 2$LiNO_3$	LDH[a] + β-$LiAlO_2$	β-$LiAlO_2$ + amorphous background	β-$LiAlO_2$ + $LiAl_5O_8$	γ-$LiAlO_2$ + $LiAl_5O_8$	γ-$LiAlO_2$ + $LiAl_5O_8$
LDH : 1LiOH	$LiAl(OH)_4{\cdot}H_2O$	α-$LiAlO_2$	β-$LiAlO_2$	γ-$LiAlO_2$	γ-$LiAlO_2$
LDH : 2LiOH	LDH + β-$LiAlO_2$	β-$LiAlO_2$ + amorphous background	β-$LiAlO_2$ + $LiAl_5O_8$	γ-$LiAlO_2$ + $LiAl_5O_8$	γ-$LiAlO_2$ + $LiAl_5O_8$

[a]LDH = $LiAl_2(OH)_7{\cdot}2H_2O$.

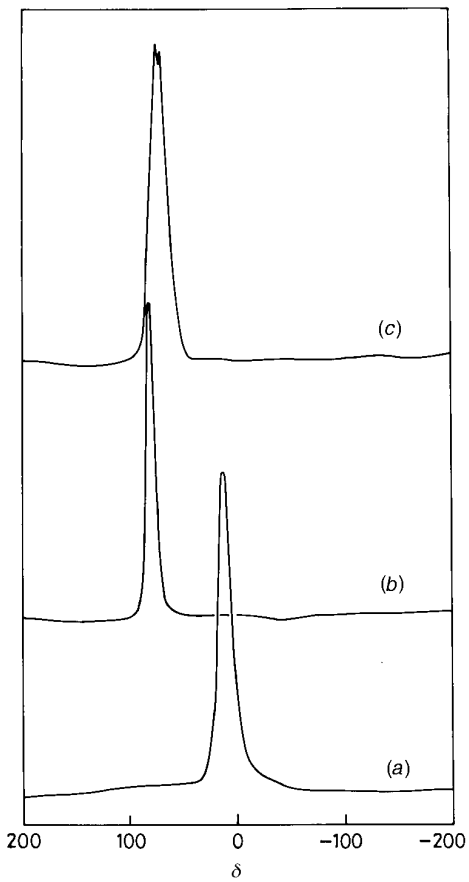

Fig. 9 Solid-state ^{27}Al MAS NMR of (*a*) α-$LiAlO_2$, (*b*) β-$LiAlO_2$ and (*c*) γ-$LiAlO_2$

in an octahedral site. By contrast, β-$LiAlO_2$ shows a chemical shift of δ 78.6 and the γ-form shows a minor splitting at δ 70 and 66. ^{27}Al chemical shifts in the range δ 50–85 are characteristic of ^{27}Al in tetrahedral sites.[25] The difference between the β and γ polymorphs is that the latter shows a clear splitting indicating site occupancy of ^{27}Al in two different types of tetrahedra, one of which may differ from the other in the degree of distortion.

The above results indicate that the two preparative techniques, G–C conversion and hydrothermal treatment, are potential routes to synthesise $LiAl_5O_8$ and $LiAlO_2$. The basic reactions in both the methods are the same; however the preparation conditions differ. Continuous influx of aliovalent ions into the gel network in the presence of hydrophilic solvents such as ethanol will bring about rapid disintegration of the gel network. Hydrophilic solvents prevent H_2O molecules re-entering into the gel network and, thereby impede the reaction. The samples prepared through G–C conversion always have very low crystallite size (0.04–1 μm), whereas hydrothermally prepared samples yield higher crystallite sizes (0.2–0.5 μm). LDH [$LiAl_2(OH)_7{\cdot}2H_2O$] prepared through the two routes differ in their characteristics although the decomposition product is the same both cases. The discrepancy may be due to the particle size and cation distribution. The differences in the particle morphology and crystallite size are further established by TEM studies.

Fig. 10 shows TEM micrographs and corresponding selected area diffraction patterns (SAED) of $LiAl_2(OH)_7{\cdot}2H_2O$ prepared *via* G–C and hydrothermal routes. The morphology and crystallite size are different in each case. The sample prepared by G–C conversion shows [Fig. 10(*a*)] fibrous needle-shaped aggregates, with particle sizes in the range 0.04–0.1 μm. SAED photographs [Fig. 10(*c*)] show spotty rings indicating the polycrystalline nature of the sample. Hydrothermally prepared samples show lamellar crystals [Fig. 10(*b*)] with sizes ranging from 0.2 to 0.5 μm and SAED [Fig. 10(*d*)] shows a spotty single crystalline pattern. The results indicate that G–C produces aggregates of fine particles, whereas hydrothermal treatment yields lamellar individual single crystallites.

$LiAl_2(OH)_7{\cdot}2H_2O$ prepared either through G–C conversion or hydrothermally acts as a precursor for the preparation of $LiAl_5O_8$. Conversion is made possible owing to Li_2O evaporation at higher temperatures, a fact not previously clarified in the literature. $LiAl_5O_8$ was also prepared from a reaction mixture having $Li_2O/Al_2O_3 = 0.22$. $LiAl_5O_8$ exists in two forms *viz.* an ordered low-temperature form and a disordered high-temperature form. The ordered form is primitive cubic ($P4_332$) while the disordered form has a true spinel structure ($F4_1/d32m$). The order–disorder transformation occurs at 1295 ± 5 °C according to the literature.[26] However, samples prepared through the present route did not undergo this type of transformation even at 1600 °C and the phase remained ordered. This indicates that the order–disorder transformation is dependent on the preparative route through which the phase is formed. When fast cooled (600 °C min^{-1}), the samples were more disordered as shown by the decreased intensity of (100) and (110) reflections in comparison with (111) and (220) reflections.

Monophasic $LiAlO_2$ was prepared hydrothermally and also by the imbibition of $LiAl_2(OH)_7{\cdot}2H_2O$ prepared through G–C conversion by $LiNO_3$ or LiOH. The structure of the LDH consists of the positively charged brucite-like layers $[LiAl_2(OH)_6]^+$ bridged by interlayer anions as well as water molecules. Depending upon the radius of the anion in the intermediate layer, the width of the interlayer varies. The existence of this intermediate layer is responsible for the unique properties of the material *viz.* anion exchange and intercalation, which makes preparation of $LiAlO_2$ possible. $LiAlO_2$ exists in different polymorphs α-, β-, and γ-$LiAlO_2$, which differ in the structure and cation coordination as established by solid-state NMR. The low-temperature form, α-$LiAlO_2$, is stable below 400 °C and is prepared *via* hydrothermal imbibition. The β-form is stable in the temperature range 500–650 °C prepared by heating the α-form at 500 °C or by hydrothermal synthesis at $\geqslant$240 °C. The compound γ-$LiAlO_2$ is prepared by heating the β-form at 1000 °C and is very stable in contrast to the material prepared *via* the sol–gel method[11] which decomposes around 600 °C to $LiAl_5O_8$ and γ-$LiAlO_2$.

Conclusions

Gel to crystallite conversion and the hydrothermal method can be easily adapted for the preparation of important materials such as $LiAl_2(OH)_7{\cdot}2H_2O$, $LiAl(OH)_4{\cdot}H_2O$, $LiAl_5O_8$ and $LiAlO_2$. The products formed are superior, in terms of homogeneity and phase content, to those prepared by conventional solid-state methods.

References

1 N. T. Melamed, F. de S. Barros, P. J. Viccaro and J. O. Artman, *Phys. Rev. B*, 1972, **5**, 3377.
2 J. G. Rabatin, *J. Electrochem. Soc.*, 1978, **25**, 920.
3 J. Van Broekhoven, *Illuminating Engineers Society Meeting*, New York, July 1, 1973.
4 M. W. Parker and H. A. Borthwick, *Plant Phys.*, 1949, **24**, 345.
5 B. Rasneuer, *Fusion Technol.*, 1985, **8**, 1909.
6 J. Jimnez-Beceril, P. Bosch and S. Bulbulian, *J. Nucl. Mater.*, 1991, **185**, 304.
7 A. J. Appleby and F. R. Foulkes in *Fuel Cell Handbook*, Van Nostrand Reinhold, New York, 1989, p. 297.
8 K. Kinoshita, J. W. Sim and J. P. Ackerman, *Mater. Res. Bull.*, 1978, **13**, 445.

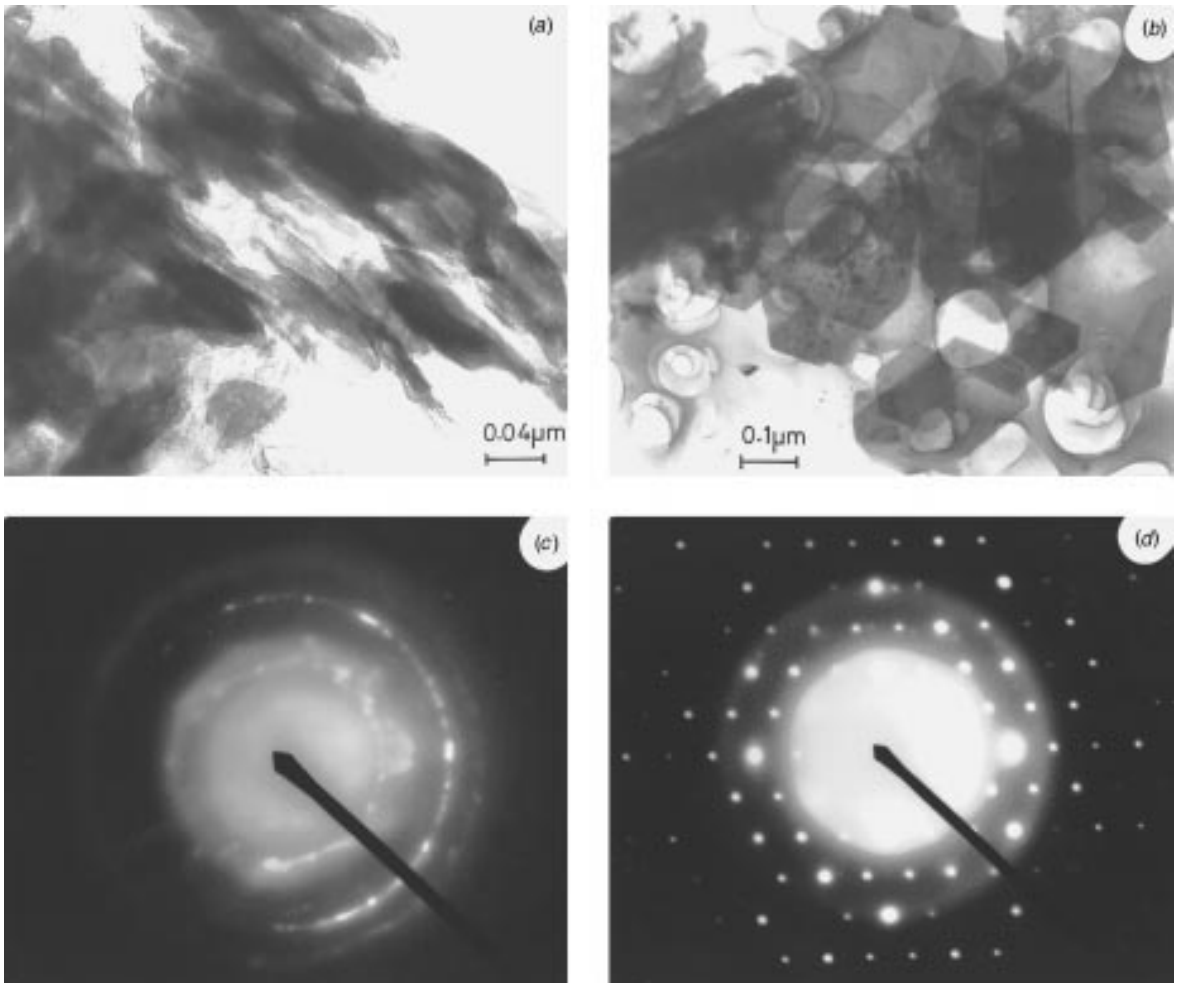

Fig. 10 TEM micrographs of $LiAl_2(OH)_7{\cdot}2H_2O$ prepared through (*a*) G–C conversion, (*b*) hydrothermal route, the white patches are due to the defect in the carbon grid used to hold the sample; (*c*) and (*d*) are SAED patterns of the samples prepared through G–C conversion and the hydrothermal method, respectively

9 K. R. Poeppelmeier, C. K. Chiang and D. O. Kipp, *Inorg. Chem.*, 1988, **27**, 4523.
10 K. R. Poeppelmeier and D. O. Kipp, *Inorg. Chem.*, 1988, **27**, 766.
11 J.-M. Jung and S.-B. Park, *J. Mater. Sci. Lett.*, 1996, **15**, 2012.
12 S. Miyata, *Clays Clay Miner.*, 1980, **28**, 50.
13 S. Miyata, *Clays Clay Miner.*, 1983, **31**, 305.
14 I. Sissoko, E. T. Eyagba, R. Sahai and P. Biloen, *J. Solid State Chem.*, 1985, **60**, 283.
15 J. E. Moneyron, A. De Roy and J. P. Besse, *Sens. Actuators B*, 1991, **4**, 189.
16 S. Miyata and A. Okaida, *Clays Clay Miner.*, 1977, **4**, 189.
17 K. R. Poppelmeir and S. J. Hwu, *Inorg. Chem.*, 1987, **26**, 3297.
18 T. R. N. Kutty and P. Padmini, *Mater. Chem. Phys.*, 1995, **39**, 200.
19 T. R. N. Kutty and M. Nayak, *Mater. Res. Bull.*, 1995, **30**, 325.
20 T. R. N. Kutty, V. Jayaraman and G. Periaswami, *Mater. Res. Bull.*, 1996, **31**, 1159.
21 T. R. N. Kutty, R. Jagannathan and R. P. Rao, *Mater. Res. Bull.*, 1990, **25**, 1355.
22 T. R. N. Kutty, *Mater. Res. Bull.*, 1990, **25**, 343.
23 C. J. Serna, J. L. Rendon and J. Iglesias, *Clays Clay Miner.*, 1982, **30**, 180.
24 M. P. Tarte, *Acad. Des. Sci.*, 1962, **254**, 2008.
25 D. Müller, G. Gessner, H. J. Behrens and G. Scheler, *Chem. Phys. Lett.*, 1981, **79**, 59.
26 K. Datta and R. Roy, *J. Am. Ceram. Soc.*, 1963, **46**, 388.

Paper 7/02065A; *Received* 25*th March*, 1997